Neuro-Oncology

Patient tumor *EGFR* and *PDGFRA* gene amplifications retained in an invasive intracranial xenograft model of glioblastoma multiforme[1]

Caterina Giannini, Jann N. Sarkaria, Atsushi Saito, Joon H. Uhm, Evanthia Galanis, Brett L. Carlson, Mark A. Schroeder, and C. David James[2]

Departments of Laboratory Medicine and Pathology (C.G., A.S., M.A.S., C.D.J.), Oncology (J.N.S., E.G., B.L.C.), and Neurology (J.H.U.), Mayo Clinic and Foundation, Rochester, MN 55905, USA

We have previously described a panel of serially transplantable glioblastoma multiforme xenograft lines established by direct subcutaneous injection of patient tumor tissue in the flanks of nude mice. Here we report the characterization of four of these lines with respect to their histopathologic, genetic, and growth properties following heterotopic-to-orthotopic (flank-to-intracranial) transfer. Cells from short-term cultures, established from excised flank xenografts, were harvested and injected into the brains of nude mice (10^6 cells per injection). The intracranial tumors generated from these injections were all highly mitotic as well as highly invasive, but they lacked necrotic features in most instances and failed to show endothelial cell proliferation in all instances. For mice receiving injections from a common explant culture, tumor intracranial growth rate was consistent, as indicated by relatively narrow ranges in survival time. In contrast to the loss of epidermal growth factor receptor gene (*EGFR*) amplification in cell culture, high-level amplification and overexpression of *EGFR* were retained in intracranial tumors established from two *EGFR*-amplified flank tumors. A third intracranial tumor retained patient tumor amplification and high-level expression of platelet-derived growth factor receptor alpha gene. Because the heterotopic-to-orthotopic transfer and propagation of glioblastoma multiforme preserves the receptor tyrosine kinase (RTK) gene amplification of patient tumors, this approach should facilitate investigations for determining the extent to which RTK amplification status influences tumor response to RTK-directed therapies. The fact that such studies were carried out by using an invasive tumor model in an anatomically appropriate context should ensure a rigorous preclinical assessment of agent efficacy. *Neuro-Oncology 7, 164–176, 2005 (Posted to Neuro-Oncology [serial online], Doc. 04-082, February 21, 2005. URL http://neuro-oncology.mc.duke.edu; DOI: 10.1215/S1152851704000821)*

Received September 3, 2004; accepted December 1, 2004.

[1] This study was supported by NCI grants CA108961 (C.G., J.N.S., J.H.U., E.G., C.D.J.), CA85779 (C.D.J.), and KO8-CA80829 (J.N.S.); NINDS grants NS49720 (C.D.J.) and K08-NS42682 (J.H.U.); American Cancer Society Research Scholar Grant RSG-03-192 (J.N.S.); and a grant from Accelerate Brain Cancer Cure (J.N.S., C.D.J.).

[2] Address correspondence to C. David James, Division of Experimental Pathology, Mayo Clinic, 200 First Street SW, Hilton Building, Room 820-D, Rochester, MN 55905, USA (james.david@mayo.edu).

[3] Abbreviations used are as follows: DMEM, Dulbecco's minimum essential media; *EGFR*, epidermal growth factor receptor gene; EGFRvIII, epidermal growth factor receptor variant III; FISH, fluorescence in situ hybridization; GBM, glioblastoma multiforme; *PDGFRA*, platelet-derived growth factor receptor alpha gene; *TP53*, p53 tumor suppressor gene.

Diffuse gliomas constitute the majority of primary brain tumors, and nearly two thirds of these are diagnosed as the most aggressive type: glioblastoma multiforme (GBM),[3] or grade IV astrocytoma (Kleihues and Cavenee, 2000). Glioblastomas are associated with high mortality and morbidity, and current therapies for their treatment have limited benefit. For these reasons,

the development of clinically relevant models for studying these tumors is essential for increasing our understanding of their biology, as well as for testing novel therapeutic approaches for their improved treatment.

For many years, immunodeficient rodents have provided an important tool used in modeling human GBM (Rana et al., 1977). Propagation and testing of GBM in such animals is most commonly accomplished in the subcutaneous flank location (heterotopic), although recent years have seen increased use of orthotopic (intracranial) xenograft models. For both heterotopic and orthotopic studies, xenograft tumors are usually established from permanent human GBM cell lines. In the orthotopic setting, established cell lines generally fail to demonstrate the diffusely infiltrative pattern of growth that is typical of human GBM; instead, they tend to form solid masses at the site of injection, which compress rather than invade the surrounding brain parenchyma (Finkelstein et al., 1994; Pilkington et al., 1997; Saris et al., 1984; Tonn, 2002). Many and perhaps most established human GBM cell lines, therefore, do not recapitulate an extremely important aspect of glioma biology (i.e., the ability to invade), and consequently the information derived from their use in an orthotopic setting has somewhat limited clinical relevance.

Glioblastoma multiforme cell lines also fail to preserve an important gene alteration that is common among GBMs: epidermal growth factor receptor (*EGFR)* gene amplification (Bigner et al., 1990; Pandita et al., 2004). In spite of a reproducible *EGFR* amplification incidence of 30% to 40% in patient GBMs (Ekstrand et al., 1991; Libermann et al., 1985; Wong et al., 1987), there exists only a single GBM cell line with stable *EGFR* amplification (Filmus et al., 1985; Thomas et al., 2001), and because this cell line is nontumorigenic, it has not been used for in vivo study. Consequently, the single most important issue regarding GBM response to Egf receptor–targeted therapeutics, whether response to therapy is influenced by tumor *EGFR* amplification status, is not approachable through the use of established GBM cell lines.

Alternative methods for establishing orthotopic GBM, such as the direct transplantation of patient surgical material into the brains of nude mice (Horten et al., 1981; Shapiro et al., 1979), have been more successful at maintaining the invasive features of these CNS tumors. Invasive orthotopic xenografts have also been established from patient surgical specimens that were first maintained as tissue spheroids in short-term culture (Engebraaten et al., 1999; Mahesparan et al., 2003). Finally, invasive intracranial tumors have been established from heterotopic xenografts generated by direct transplantation of patient surgical specimens and subsequently sustained by serial passaging in the flanks of nude mice (Antunes et al., 2000; Taillandier et al., 2003).

Continuous serial passaging of flank tumors also preserves patient tumor gene alterations, including *EGFR* amplification (Leuraud et al., 2003; Pandita et al., 2004). Here we report on the morphologic and genetic properties of intracranial tumors established from xenografts maintained via serial passaging in the flank. The preservation of tumor *EGFR* amplification status as well as tumor invasiveness in the orthotopic setting, when combined with a short-term cell culture step that facilitates the injection of a constant number of tumor cells in several mice, supports this model as being highly amenable to assessing GBM therapeutic response as a function of tumor *EGFR* amplification status.

Material and Methods

Clinical Information

Tumors used in this study were obtained from patients who were undergoing surgical treatment at the Mayo Clinic in Rochester, Minnesota, and who had consented to the use of their tissue for research. Tumor imaging in these patients was performed with a head coil on a 1.5-tesla clinical MR scanner (General Electric, Waukesha, Wis.), and images were obtained by using a standard T1 protocol following gadolinium injection. Following intraoperative surgical pathology consultation confirming the suspected clinical diagnosis of GBM (Kleihues and Cavenee, 2000), excess fresh tissue was collected for heterotopic (flank) injection into nude mice. Upon review of permanent sections, all tumors were diagnosed as grade IV astrocytomas that displayed the typical morphologic features of GBM, including presence of mitotic activity, endothelial vascular changes, and necrosis (see Table 1 and Fig. 1).

Table 1. Patient clinical data

Patient	Age/Sex	Tumor Site	Pathology	RT Dose (cGy)	Survival (months)	Cause of Death
5	57/M	Rt temporal	Fibrillary and gemistocytic	6000	31	Tumor recurrence
6	65/M	Lt frontal	Small cell	6000	13	Tumor recurrence
12	68/M	Lt occipital	Fibrillary	6120	3*	Pulmonary embolism
14	56/M	Rt temporal	Fibrillary	6120	11	Tumor recurrence

Abbreviations: Lt, left; Rt, right; RT, radiotherapy.

*Death at three months was attributable to acute pulmonary embolism rather than to tumor, as there was no evidence of recurrent tumor by MRI analysis conducted just prior to the time of death.

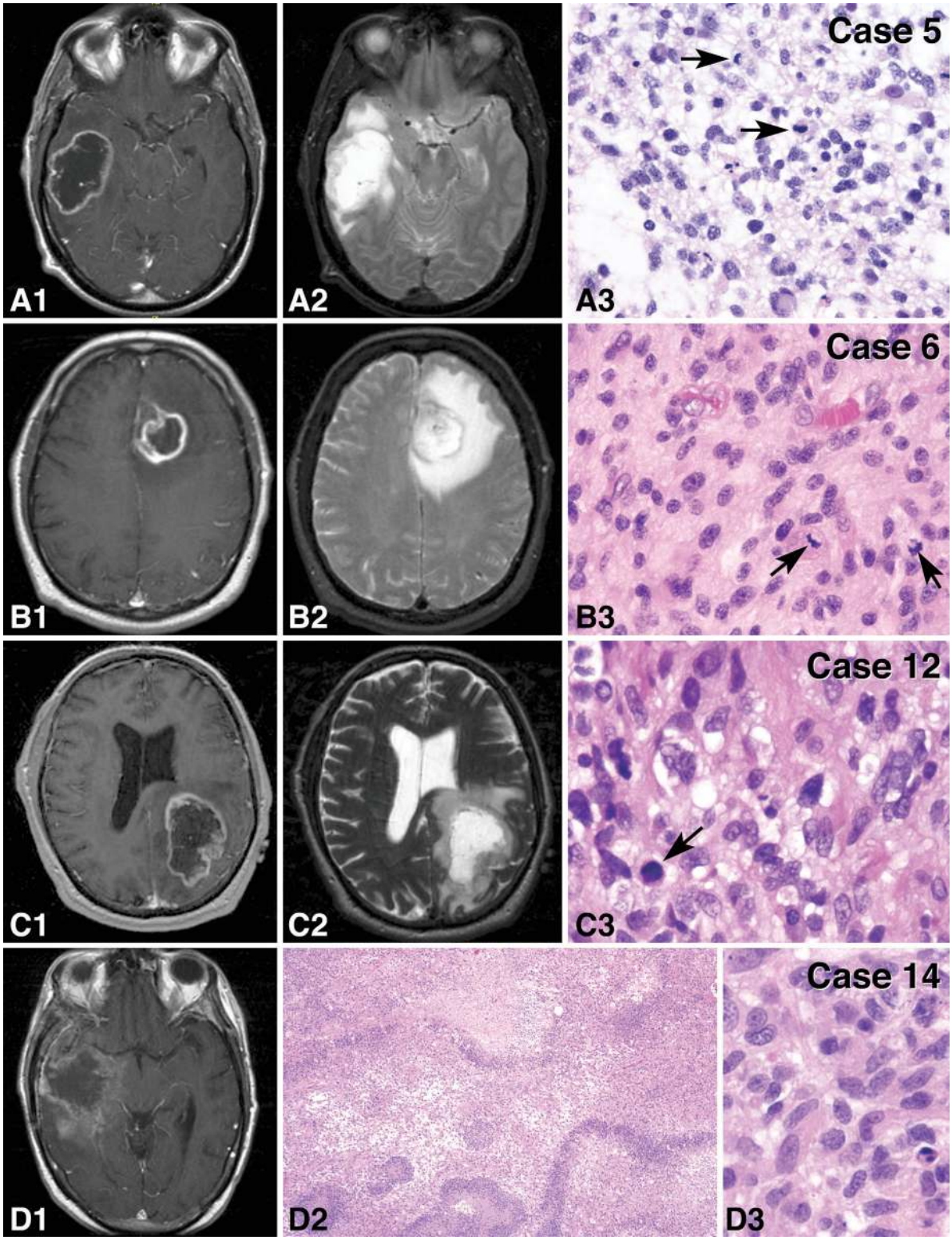

Fig. 1. MRI and histopathologic features of the patient tumors used to establish the xenograft lines. For cases 5, 6, and 12, both T1 with contrast (A1–C1) and T2 (A2–C2) sequences show features prior to the first surgery; for case 14, the T1 with contrast image (D1) was obtained at time of tumor recurrence. All MRI images revealed large, irregular, nonhomogeneous, peripherally enhancing masses surrounded by marked edema. Histopathologically, the tumors were composed of neoplastic astrocytes with varying appearance (A3–D3). Tumor morphologies included a mixture of fibrillary astrocytes and pleomorphic cells having relatively abundant cytoplasm (case 5, panel A3), small cell morphology (case 6, panel B3), and fibrillary astrocytes (cases 12 and 14, panels C3 and D3, respectively). All tumors were mitotically active (arrows, A3–C3), and all tumors showed evidence of necrosis, as exemplified in panel D2 for case 14. H&E, ×10 (D2) and ×40 (A3–D3).

Heterotopic and Orthotopic Tumor Propagation

Congenitally athymic nude mice, five to eight weeks old (Charles River Laboratories, Wilmington, Mass.), were used throughout this study in accordance with federal and institutional guidelines. For initial heterotopic establishment of the xenograft lines, excised patient tissue was placed in a culture dish with Dulbecco's minimum essential media (DMEM) and minced into small pieces, such that minced tissue suspensions could be drawn through a 16-gauge needle. Minced tissues were placed in a conical tube, media was withdrawn, and Matrigel (BD Biosciences, Franklin Lakes, N.J.) was added to the wet tissue in a 1:1 volume ratio. Next, 200 μl of the Matrigel-tissue mixture was injected subcutaneously into the flanks of two to four mice, and tumors were allowed to develop until they reached a length of 1.0 to 2.0 cm in longest dimension. At that time the mice were sacrificed by CO_2 asphyxiation, and their flank tumors were immediately excised. Portions of each excised flank tumor were archived as frozen tissue and as paraffin-embedded tissue following formalin fixation. The remainder of each tumor was dispersed in DMEM, processed as before, and passaged by injection into the flank of another nude mouse.

Flank tumor passages 5, 10, 5, and 4 were used for establishing intracranial tumors from GBMs 5, 6, 12, and 14, respectively, and 490, 585, 725, and 418 days, respectively, were required to obtain these flank tumor passages (from date of initial flank injection of corresponding patient tumor tissue). To prepare cells for transfer to the intracranial compartment, the excised flank tumors were placed in culture dishes, where the tissue was initially minced with a scalpel and then mechanically disrupted by repetitive pipetting to create a cell suspension. Following short-term culture of the tumor cells (three to seven days) in DMEM with 2.5% fetal calf serum, cells were trypsinized, washed 2× in phosphate-buffered saline, then resuspended in phosphate-buffered saline at 10^5 cells/μl and kept on ice until injected intracranially into four or five mice with a Hamilton syringe (Hamilton Company, Reno, Nev.). For this procedure, the calvarium of each anesthetized mouse was exposed through a midline incision, and a burr hole was drilled 1 mm lateral (right) and 2 mm anterior to the bregma. With the aid of a small animal stereotactic frame (ASI Instruments, Houston, Tex.), cells were injected at a rate of 1 μl/min for 10 min (total of 10^6 cells injected per mouse), with the syringe left in place for 10 min following completion of tumor cell injection. Injections were to a depth of 3 mm below the outer table of the skull, thereby introducing the tumor cells near the right caudate nucleus. Following tumor cell injection, mice were observed daily until they reached a moribund state, at which time they were euthanized and their brains removed and processed for histopathologic analysis. Analysis of intragroup variation in length of survival included standard deviation and 95% confidence interval determinations.

Tissue Processing for Morphologic and Molecular Analysis

Prior to removal of whole brains with xenograft tumor for histopathologic processing, mice were euthanized by cardiac perfusion with paraformaldehyde while under deep anesthesia. Whole brains were fixed by overnight immersion in formalin, and the fixed specimens were subsequently embedded in paraffin and then sectioned according to routine pathological procedures. Sectioned tissues were deparaffinized and then hydrated in distilled water. Hydrated sections were immersed in hematoxylin for 3 min, rinsed in distilled water until clear, immersed in bluing reagent (Richard-Allan Scientific, Kalamazoo, Mich.) for 1 min, washed with tap water for 5 min, immersed 10× in 95% alcohol, counterstained with eosin for 45 s, immersed 10× in 95% alcohol and 10× in absolute alcohol, and finally cleared with two changes of xylol prior to mounting.

Immunohistochemical Analysis

Formalin-fixed, paraffin-embedded sections were immunostained for total Egf receptor protein by using mouse monoclonal antibody 528 (Oncogene Research Products, San Diego, Calif.), as previously described (Aldape et al., 2004). Staining for epidermal growth factor receptor variant III (EGFRvIII) protein was accomplished with microwave antigen retrieval in 10 mM sodium citrate, pH 6.0, followed by the cooling of tissue sections to room temperature prior to adding rabbit polyclonal antibody against EGFRvIII protein (1:300 dilution; Zymed, South San Francisco, Calif.), with subsequent overnight incubation at 4°C (Aldape et al., 2004). Staining was visualized by use of the Dako Envision kit (Carpinteria, Calif.) according to the manufacturer's instructions. The p53 immunohistochemistry, which has been described previously (James et al., 1999), involved utilization of the p53 antibody DO-7 (Dako).

Analysis of Nucleic Acids Extracted from Tissues

High-molecular-weight DNA was isolated from patient tissues and their corresponding flank tumor xenografts as previously described (James et al., 1988). We examined the DNA from each patient tumor and from at least five flank tumors of each xenograft line for amplification of *EGFR* and platelet-derived growth factor receptor alpha (*PDGFRA*) by Southern blot analysis (as described in Galanis et al. [1998]), for homozygous deletion of *CDKN2A* by multiplex PCR (as described in James et al. [1999]), and for mutation of *PTEN* as well as p53 tumor suppressor gene (*TP53)* by sequence analysis of PCR-amplified genomic fragments (James et al., 1999). Isolation of RNA and subsequent analysis of gene expression by Northern blot was as previously described (Wang et al., 1998).

FISH Analysis

Fluorescence in situ hybridization (FISH) for *EGFR* and *PDGFR* amplification was performed on paraffin

sections from intracranial xenografts. *EGFR* and chromosome 7 centromeric probes, or *PDGFR* and chromosome 4 centromeric probes, were labeled with Spectrum orange and Spectrum green (Vysis, Downers Grove, Ill.), respectively, and hybridized to tissue sections as described previously (Pandita et al., 2004; Smith et al., 2000). Tissues lacking *EGFR* and *PDGFRA* amplifications showed target-to-centromere signal ratios at or near 1, whereas tissues with amplifications revealed target-to-centromere signal ratios substantially greater than 1. In all instances, the gene amplification status for intracranial paraffin-embedded tissues (assessed by FISH) and that for the corresponding flank genomic DNA (assessed by Southern analysis) were in agreement.

Results

Patient Clinical Information

The four xenograft lines examined here were established from grade IV astrocytomas, and the clinical history of each was consistent with primary or de novo GBM. Patient data, including tumor morphologic and imaging features, are presented in Table 1 and Fig. 1. All patients were male and had been treated by debulking surgery resulting in gross subtotal tumor resection, and each received standard fractionated radiation therapy (6000 or 6120 cGy); one patient (patient 5) additionally received adjuvant BCNU (bis-chloroethylnitrosourea) chemotherapy. Tumors used to establish xenografts 5, 6, and 12 were obtained at the time of initial surgery, whereas xenograft 14 was obtained during a second surgical procedure at time of tumor recurrence, and following radiation therapy. Survival from initial surgeries varied from 3 to 31 months.

Morphology and Histopathology of Flank Xenografts

Heterotopic xenografts, maintained by serial transplantation in the flanks of nude mice, retained histopathologic features similar to those of the patient GBMs from which they were established and included the presence of necrosis (Fig. 2). Of 128 flank tumors, 107 (83.6%) showed evidence of necrosis, and the extent of necrosis appeared to be proportional with increasing flank tumor size. Endothelial proliferation, with multilayering of endothelial cells (three to four layers), was not observed in any flank tumor; mild microvascular proliferation was observed in just one instance (GBM 14, Fig. 2).

Morphology, Histopathology, and Growth of Intracranial Tumors Established from Flank Xenografts

After multiple heterotopic passages, flank tumors were excised and mechanically dissociated in cell culture media. Following short-term in vitro growth, cells from each xenograft explant culture were harvested and injected into the brains of four to five mice (all mice receiving 10^6 cells). Differences in length of survival (from time of injection to reaching a moribund state) were limited to a few days among mice receiving injections with the same xenograft cell preparation (Table 2). Two of the xenografts, 12 and 14, showed similar and rapid rates of intracranial growth, whereas xenograft 5 was particularly slow to produce symptoms indicative of intracranial tumor burden. Interestingly, the patient with this tumor survived 31 months, much longer than the other three patients (Table 1) and well beyond the median survival (10–12 months) of GBM patients as a whole.

Examination of whole brain sections from mice receiving intracranial tumor cell injections revealed tumor features consistent with high-grade astrocytoma in all instances (Figs. 3 and 4). Each tumor showed indication of an advanced stage of growth and displayed an area of high cellular density at the site of intracranial injection that was surrounded by an ample front of invasion into surrounding parenchyma (Fig. 3). In many respects, intracranial xenograft tumors displayed a close resemblance to the respective patient tumors (Fig. 1), although there was a tendency for the tumor cell composition of the intracranial xenografts to appear more homogeneous.

The mitotic activity of the xenograft tumors was considerably higher than that of corresponding patient tumors (>3× in all instances), whereas the mitotic indices of corresponding flank and intracranial tumors were similar, showing mean values of 11.6 versus 10.7, 12.2 versus 10.0, 25.8 versus 24.4, and 13.7 versus 10.6 per high-powered field (flank vs. intracranial), for GBMs 5, 6, 12, and 14, respectively. Unlike that seen in the corresponding flank and patient tumors, necrosis in intracranial tumors was uncommon, with only a few instances of focal necrosis observed among the intracranial xenograft tumors: in two of five GBM 12 (see Fig. 3, C1 and C2) and in one of four GBM 6 intracranial tumors, but not in any of four GBM 5 or in any of four GBM 14 intracranial tumors. Finally, no endothelial hyperplasia or endothelial proliferation was observed in any of the intracranial xenografts (see Discussion).

In all intracranial xenografts, tumor cell clusters as well as isolated tumor cells could be observed infiltrating surrounding parenchyma with distant extension away from the main tumor mass (Fig. 4). Reflecting their invasive behavior in the patient setting, tumor cells injected into the rodent brain were observed as migrating along white matter fibers of the corpus callosum, as well as through the anterior commissure, leading to tumor dissemination to the contralateral hemisphere (Fig. 4, GBM 6 and GBM 12). Infiltration of adjacent cortex and basal ganglia was also evident. In all intracranial GBM xenografts, tumor cells reaching the cortical surface extended into the overlying subarachnoid space, in some cases giving rise to diffuse leptomeningeal spread (Fig. 4, GBM 14, right panel). Intraventricular tumor spread was also observed, with tumor extensions seeding the lateral and third ventricles (Fig. 4, GBM 14, center panel), as well as the sylvian aqueduct (Fig. 4, GBM 6, left panel inset); these intraventricular tumor cells typically formed tumor nodules (Fig. 4, GBM 14, left and center panels). Infiltrative tumor cell behavior was most pronounced in tumors established from GBM 5, which demonstrated a widespread dissemination through all

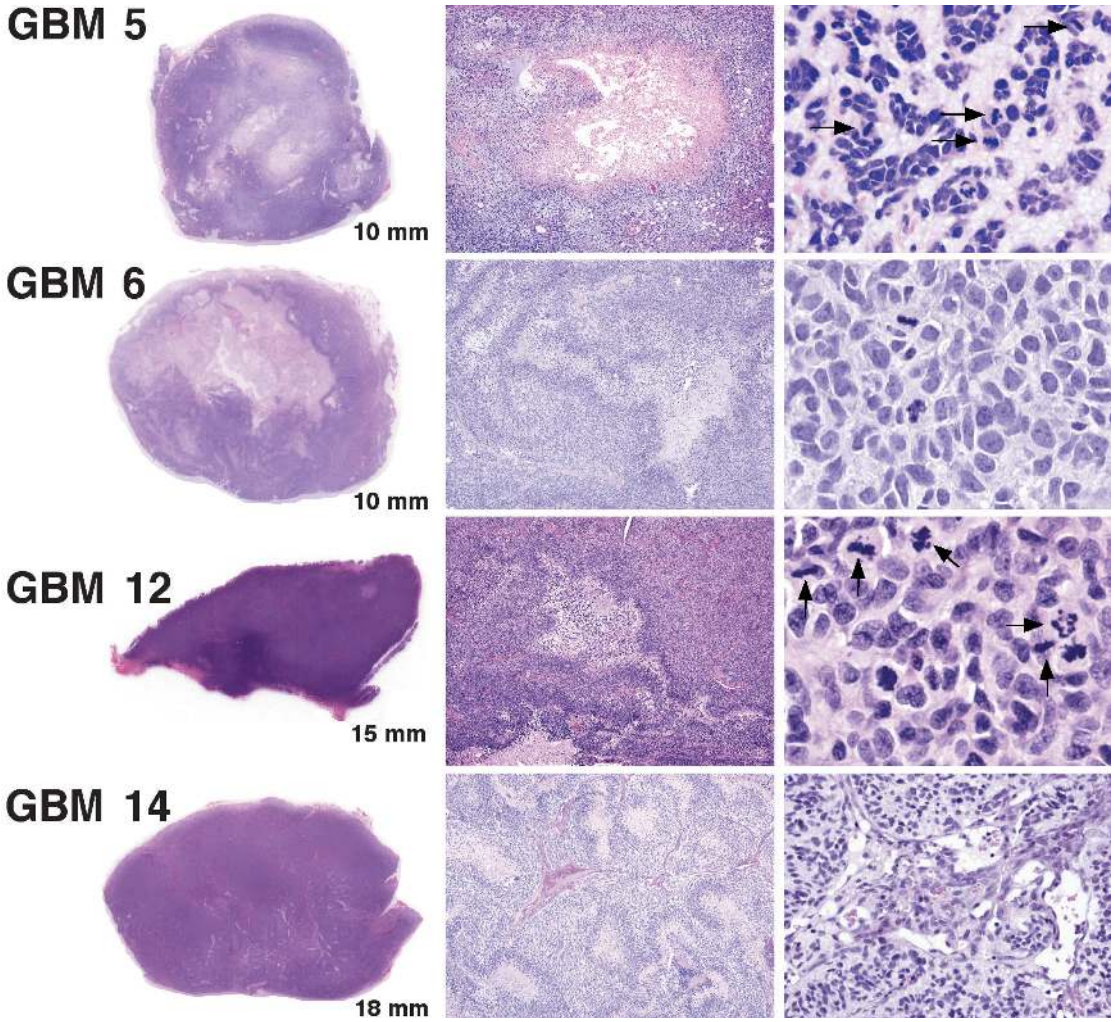

Fig. 2. Flank tumor histopathology. Scanned images of H&E-stained sections from resected flank tumors, which grow as relatively solid demarcated nodules in subcutaneous tissue, are shown in the panels to the left (longest distance across each specimen is indicated in the lower right corner of each image). The specimen for GBM 12 shows a rare instance of flank tumor focal invasion of the abdominal musculature (lower left edge). Most flank tumors, as illustrated in the middle panels (4× magnification), show necrotic regions similar to those seen in the original GBMs from which they were derived. Pseudopalisading surrounding areas of necrosis are evident in GBMs 6 and 14. In the images shown to the right (40× magnification), flank tumor recapitulation of corresponding patient tumor morphology is evident. In the GBM 5 specimen, a "mucoid/myxoid" intercellular matrix is shown (see also Fig. 1, A3). Note the high cellularity and mitotic activity (arrowheads) in the GBM 5 and 12 specimens. For the GBM 14 specimen, a rare instance of early microvascular change is displayed (right panel).

Table 2. Survival interval[1] following intracranial injection of xenograft cells

	M1	M2	M3	M4	M5	SD (days)	95% CI (days)
GBM 5	154	159	113	159	-	22.3	110.8–181.7
GBM 6	49	32	49	52	-	9.1	31.0–60.0
GBM 12	31	31	31	34	34	1.5	29.4–34.1
GBM 14	33	28	33	33	-	2.5	27.8–35.7

Abbreviations: CI, confidence interval; GBM, glioblastoma multiforme; SD, standard deviation.

[1]Days from injection of 10^6 cells to mouse becoming moribund.

the brain parenchyma and the brain stem, and which displayed an extent and pattern of infiltration similar to that seen in gliomatosis cerebri (Fig. 4).

Molecular Analysis of Intracranial Xenograft Tumors

Previously we have shown that GBM 6 and 12 flank tumors contain amplified and overexpressed *EGFR*, whereas flank tumors from xenografts 14 and 5 do not have this genetic alteration (Pandita et al., 2004). Although it is seemingly implicit that gene alterations are stably transmitted during tumor propagation, we have demonstrated that amplified *EGFR* is not retained by xenograft cells continuously grown in cell culture (Pandita et al.,

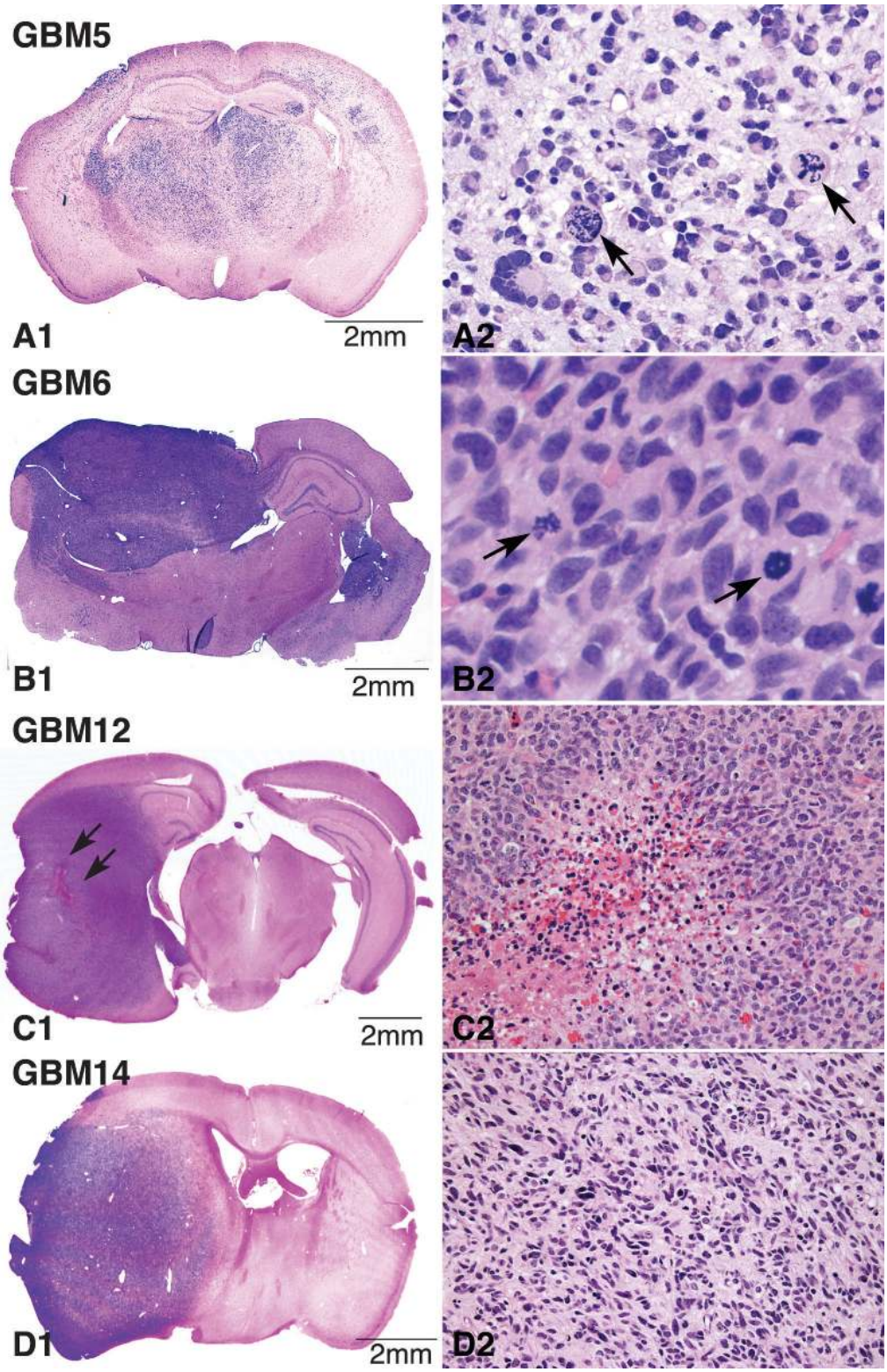

Fig. 3. Growth patterns of intracranial xenografts in full coronal section (left) and corresponding morphologic features of neoplastic cells in areas of maximal tumor density (right). All intracranial xenografts show areas at the site of injection that are characterized by high cellularity and at which the tumor appears virtually solid. Note the close resemblance between the morphology of the xenograft tumor cells and the cells in their corresponding patient tumors (Fig. 1). For the GBM 12 example, a small focus of hemorrhagic necrosis is shown (indicated in C1 by arrows and at higher magnification in C2), and the beginning of pseudopalisade formation is evident (C2). H&E: A2 ×20, B2 ×40; C2, D2 ×10. Arrows (panels A2 and B2) denote mitotic figures.

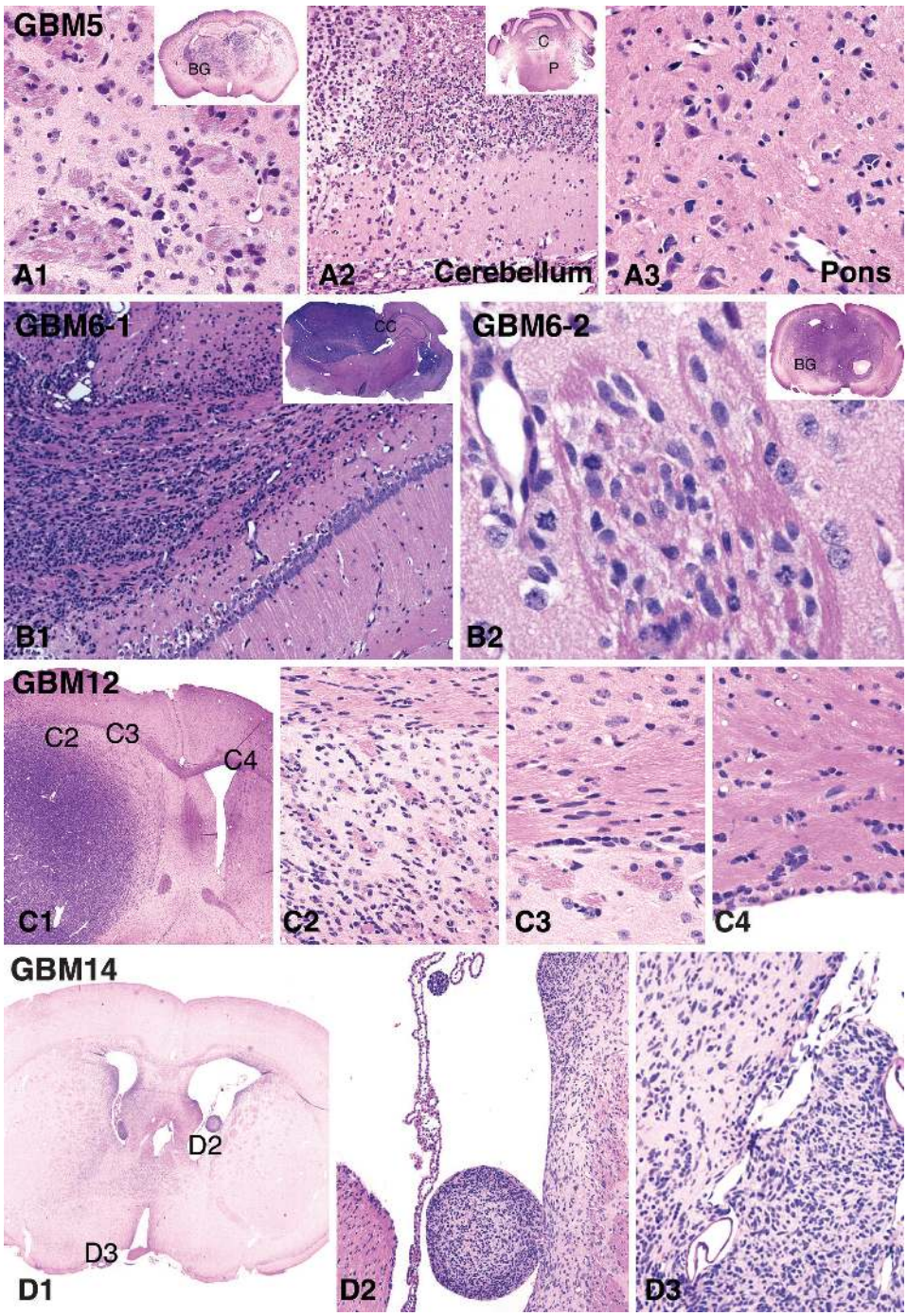

Fig. 4. Highly invasive characteristics of intracranial tumors generated from flank xenografts. GBM 5 intracranial tumors showed widespread infiltration of all brain parenchyma, resulting in a morphology similar to that of gliomatosis cerebri. This tumor reaches its highest cellularity and approaches a nearly solid appearance in the most rostral section near the site of injection, although tumor cells were readily apparent in all sections examined. As shown here, single tumor cells can be seen infiltrating the basal ganglia (panel A1 and indicated as "BG" in the inset), the molecular layer of the cerebellar cortex (panel A2 and indicated as "C" in the inset), and the pontine base (panel A3 and indicated as "P" in the inset of panel A2). In a GBM 6 intracranial tumor, a large number of tumor cells can be seen migrating through the corpus callosum (panel B1 and indicated as "CC" in the inset) and extending into the opposite hemisphere. For a second GBM 6 intracranial tumor (panel B2 and inset), a region of neoplastic cells infiltrating the basal ganglia (BG) and extending along perivascular spaces, as well as along pencil fibers, is shown. In an example of a GBM 12 intracranial xenograft tumor (C1), single tumor cells can be seen infiltrating adjacent gray and white matter (C2), aligning along white matter tracts that converge into the corpus callosum (C3), and crossing the midline into the opposite hemisphere (C4). Diffuse infiltration is also evident in the example of GBM 14 intracranial xenograft tumor, which shows crowding of neoplastic cells in the immediate periventricular areas on both sides (D1), with extension into the ventricles readily apparent because of the presence of intraventricular tumor nodules (D2). In the same GBM 14 tumor, leptomeningeal extension is recognizable along the interhemispheric fissure (D3). H&E, magnifications vary from ×4 to ×40.

2004). Thus, the selection for high-level amplification-associated expression of Egf receptor is influenced by the local environmental context in which the tumor cells are propagated. Here, our immunohistochemical and FISH analysis demonstrated consistency of *EGFR* amplification and expression status, between the flank and intracranial settings, for all xenografts (Fig. 5).

In addition to *EGFR* amplification, xenografts 6 and 12 harbor *TP53* mutations. For the former, a missense mutation at codon 273 results in increased stability of tumor cell p53 protein, leading to highly positive immunohistochemical staining. For xenograft 12, a *TP53* gene splice site mutation results in a lack of immunohistochemically detectable p53 protein (Fig. 5).

GBM 5 flank tumors had been previously determined as having amplification of another growth factor receptor gene important to the biology of malignant glioma: *PDGFRA*. Results from FISH analysis of GBM 5 intracranial tumors, established from a flank tumor with amplification-associated, high-level *PDGFRA* expression (Fig. 6, right), showed orthotopic tumor retention of amplified *PDGFRA* (Fig. 6, upper left). A summary of gene alterations identified in corresponding patient tumors, flank tumors, and intracranial tumors is shown in Table 3.

Discussion

Glioblastoma multiforme is a highly invasive tumor, and this characteristic certainly contributes to the failure of current therapies aimed at trying to control this aggressive malignancy. Most established GBM cell lines form discrete, noninvasive tumors with well-circumscribed borders that push aside rather than invade adjacent normal tissue (Finkelstein et al., 1994; Mahesparan et al., 2003; Pilkington et al., 1997; Saris et al., 1984; Tonn, 2002). This lack of invasiveness may limit the clinical relevance of studies assessing the efficacy of novel therapies when tested against intracranial tumors established from noninvasive GBM cell lines.

In contrast to the established cell lines, all of the xenograft lines we have tested in the orthotopic (intracranial) setting form highly invasive tumors that show widespread dissemination, infiltration along white matter tracts, seeding of the ventricular system, and even extension along the leptomeninges (Figs. 3 and 4). Because GBMs that have been continuously propagated as flank tumors recapitulate this very important and characteristic feature of human GBM following intracranial transfer, the heterotopic-to-orthotopic tumor propagation model should provide a more relevant

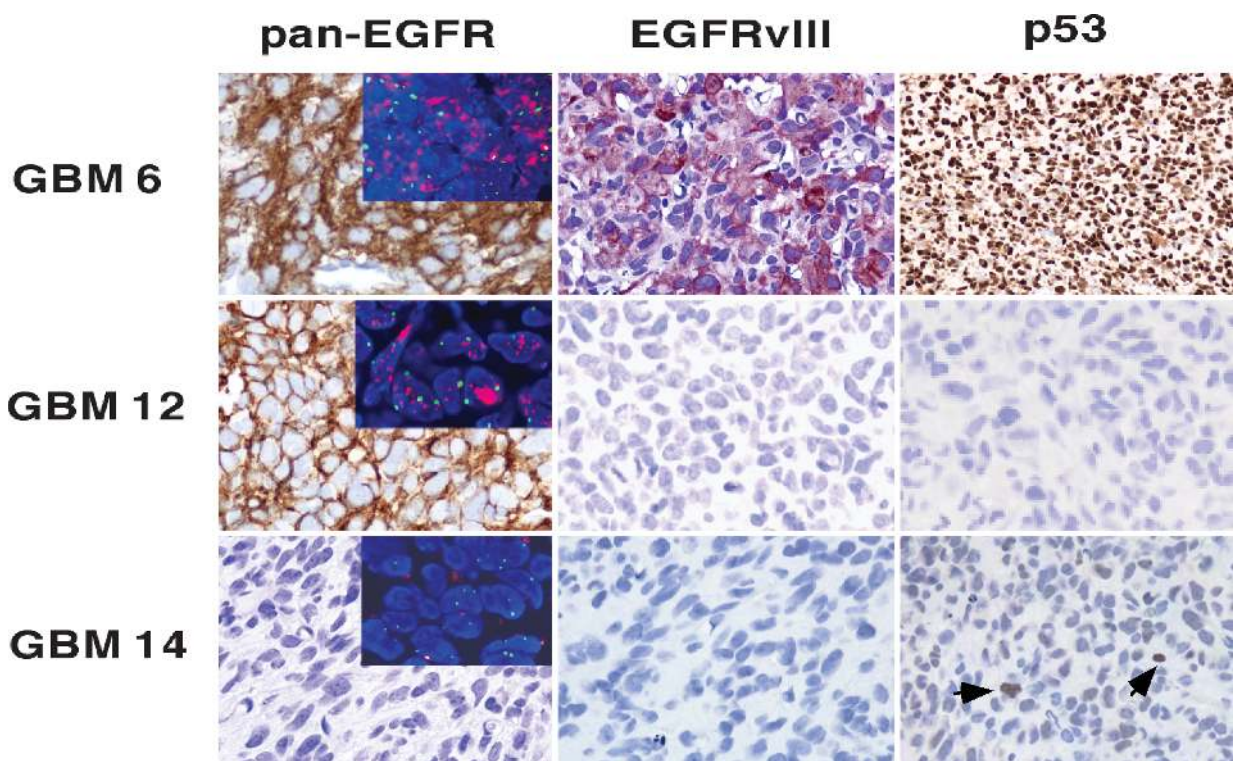

Fig. 5. Intracranial tumor retention of genetic characteristics previously determined in corresponding flank tumors. Pan-EGFR: Ab 528 (Clontech), which recognizes both wild-type and vIII mutant Egf receptor. EGFRvIII: Zymed polyclonal antibody specific for vIII mutant EGFR. p53: results from use of DO-7 Ab (Dako), which recognizes wild-type and missense mutants of p53. GBM 6 stains intensely positive with this latter antibody because of the presence of a stabilizing p53 mutation. GBM 12 is negative for p53 staining because of a splice mutation preventing the synthesis of reactive p53 protein. GBM 14, with wild-type p53, shows occasional, weakly positive cells (arrowheads). Inset pictures in the panels at the left show the results of FISH analysis with fluorescent probes for *EGFR* (red) and chromosome 7 centromere (green); these images reveal numerous and merged *EGFR* signals, indicative of *EGFR* amplification, in cells from GBMs 6 and 12 but not from GBM 14.

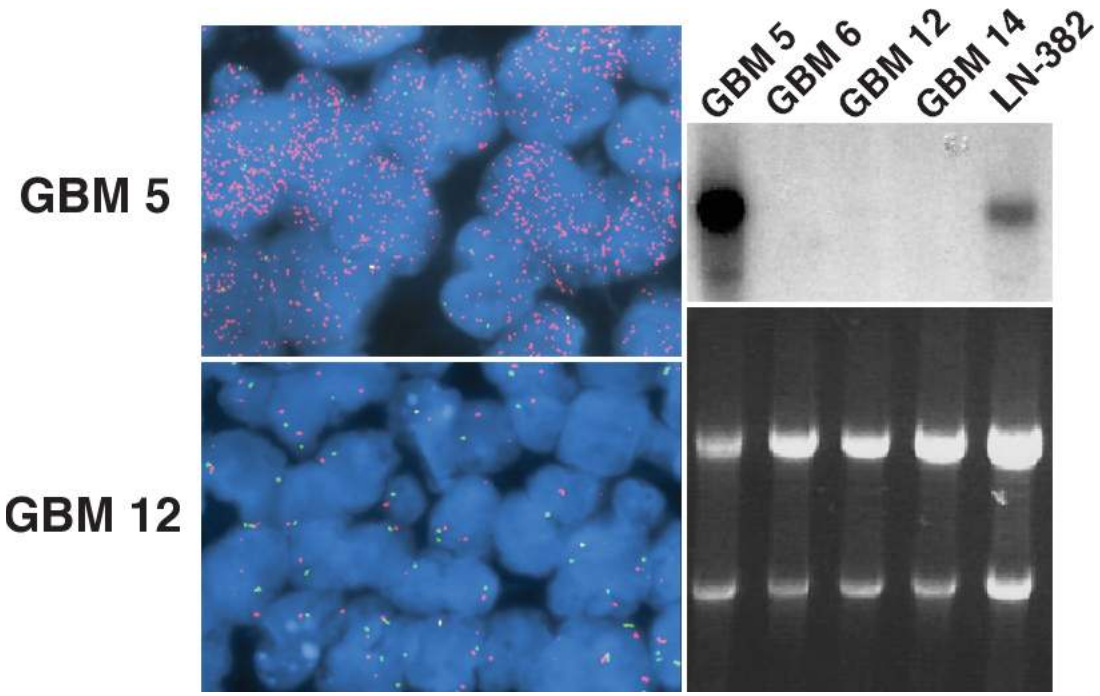

Fig. 6. Maintenance of *PDGFRA* amplification in intracranial tumors established from *PDGFRA*-amplified flank tumor. Upper left. *PDGFRA* FISH result for intracranial GBM 5 showing high-level *PDGFRA* copy number (*PDGFRA* = red signal; green signal = chromosome 4 centromere probe). Lower left. Results for GBM 12 intracranial tumor, which lacks amplified *PDGFRA*, are shown for comparison. Upper and lower right panels. *PDGFRA* Northern blot (upper panel) and corresponding RNA gel (lower panel) showing extent of sample loading variation via 28S and 18S ribosomal RNA signal intensity. The autoradiogram image in the upper right panel shows high-level *PDGFRA* expression in GBM 5 flank xenograft. The GBM cell line LN-382, previously determined as having amplified *PDGFRA*, also shows detectable *PDGFRA* transcript. The level of *PDGFRA* expression in all other specimens shown here is beneath the level of detection for the length of film exposure used.

system for preclinical assessment of novel therapeutic agents, especially for those agents targeting the invasive phenotype of GBM (Groves et al., 2002).

Although this approach to tumor propagation preserves invasive growth, it is important to emphasize that these intracranial tumors generally do not display necrosis and have not shown any endothelial proliferation. Because necrosis was observed in most flank tumors from which the intracranial tumors were derived, and because the flank tumors can be grown to substantially larger volumes than their corresponding intracranial tumors, our results suggest that the development of necrosis could well be dependent on the tumor having achieved sufficient size. This hypothesis could be tested via tumor propagation in an animal with a larger intracranial volume, such as a nude rat. Indication of endothelial cell proliferation, on the other hand, was observed in only a single flank tumor and was not observed in any intracranial tumors, thereby suggesting a limited ability of human GBM cells to stimulate proliferation of mouse endothelial cells.

Our methodology for establishing orthotopic xenografts includes the mechanical dispersion of cells from flank tumors in cell culture media, followed by short-term (<1 week) in vitro tumor cell expansion prior to harvest and subsequent intracranial injection. This aspect of the procedure permits the accurate and repeated delivery of a specified number of tumor cells via a minimally invasive and easily reproducible surgical technique: a limited scalp incision and a burr hole for stereotactic tumor cell inoculation. Tumors established with this technique show a consistent rate of growth, as indicated by the relatively narrow ranges in time for the presentation of severe neurologic symptoms among series of mice receiving injection of a common cell preparation (Table 2). Data from repeat experiments with these xenografts indicate that interexperimental variation in length of time required for the development of neurologic symptoms, when using a specific xenograft line, is minimal. These results, in turn, suggest that pilot data collected on intracranial growth rates can be used to predict the time to onset of neurologic symptoms with a high degree of accuracy and therefore can be used to plan the timing of the administration of experimental therapies. Finally, intracranial tumor engraftment using this technique has been 100%, and we have experienced an extremely low procedure-related mouse mortality (<1%).

Two other groups have reported the use of serially passaged flank GBM xenografts for establishing intracranial tumors (Antunes et al., 2000; Bernsen et al., 1999). In the initial report from one of these groups (Antunes et al., 2000), only a broad range in time to death was indicated for mice receiving intracranial tissue implants from specific flank xenografts. That is, survival times for individual mice were not reported, thereby precluding determination of the consistency of tumor growth rate by this procedure. It seems likely that the broad range in

Table 3. Comparison of gene alterations detected in corresponding patient, flank xenograft, and intracranial xenograft tumors

	Gene Alterations[1, 2]				
Tumor[3]	*EGFR*	*PDGFRA*	*TP53*	*PTEN*	*CDKN2A*
5_p	$-^{sb,f}$	$+^{f}$	$-^{s}$	$-^{s}$	$-^{PCR}$
5_f	$-^{sb,f}$	$+^{sb,f}$	$-^{s}$	$-^{s}$	$-^{PCR}$
5_i	$-^{f}$	$+^{f}$	$-^{IHC}$	ND	ND
6_p	$+^{sb,f}$	$-^{f}$	$+^{s}$	$-^{s}$	$+^{PCR}$
6_f	$+^{sb,f}$	$-^{sb,f}$	$+^{s}$	$-^{s}$	$+^{PCR}$
6_i	$+^{f}$	$-^{f}$	$+^{IHC}$	ND	ND
12_p	$+^{sb,f}$	$-^{f}$	$+^{s}$	$-^{s}$	$+^{PCR}$
12_f	$+^{sb,f}$	$-^{sb,f}$	$+^{s}$	$-^{s}$	$+^{PCR}$
12_i	$+^{f}$	$-^{f}$	$+^{IHC}$	ND	ND
14_p	$-^{sb,f}$	$-^{f}$	$-^{s}$	$-^{s}$	$+^{PCR}$
14_f	$-^{sb,f}$	$-^{sb,f}$	$-^{s}$	$-^{s}$	$+^{PCR}$
14_i	$-^{f}$	$-^{f}$	$-^{IHC}$	ND	ND

[1]Alterations were as follows: amplifications of *EGFR* and *PDGFRA*; mutations of *TP53* and *PTEN*; and deletion of *CDKN2A*.

[2]Superscripts denote method of analysis used: f = fluorescence in situ hybridization; IHC = immunohistochemistry; ND = not determined; PCR = polymerase chain reaction; s = sequencing; sb = Southern blot. All flank tumor entries are based on the analysis of at least five tumors for each xenograft line, with consistent results obtained between flank tumors for each gene alteration that is indicated. The intracranial tumor entries in this table are based on the analysis of all intracranial tumors from the mice indicated in Table 2, with consistent results obtained for each gene alteration that is indicated for each xenograft line.

[3]Subscripts denote tumor source: p, patient; f, flank xenograft; i, intracranial tumor.

survival time that was indicated reflects the use of tissue, rather than dispersed cells, for orthotopic implantation. One might expect such an approach to have inherent variation between mice in the quantity and/or viability (e.g., necrosis) of implanted tumor cells.

A second group that has used the flank-to-intracranial tumor propagation approach (Bernsen et al., 1999) developed cell suspensions from flank xenografts as a source of material for intracranial injection. Whereas one might anticipate this procedural variation to reduce differences in the quantity of viable tumor cells delivered to each animal, the length of survival for athymic rats having received injections was not an objective of the study, so no survival data were reported. Finally, an approach bearing some similarity to the one reported here, involving short-term culturing of tumor spheroids established from single GBM patient specimens and subsequently injected into the brains of nude rats, has also been reported (Engebraaten et al., 1999). Since rats receiving tumor spheroid intracranial injections were all sacrificed at a common time subsequent to the injection procedure, length of survival was not an objective of this study either. The authors of this report did, however, indicate substantial variations in size of developing intracranial tumors that were evident at the time of sacrifice. In the procedure described here, we have shown that the quantitatively uniform delivery of viable tumor cells from short-term flank xenograft explant cultures allows one to establish intracranial tumors in series of mice, amongst which intra-group differences in extent as well as rate of tumor development are minor.

The genetic characterization of flank xenografts is another key aspect of our model that should facilitate testing of therapeutic as well as biological hypotheses. For instance, here we have shown two examples of GBM xenografts consisting of tumor cells with both amplified *EGFR* and *TP53* mutation. Previous studies of patient surgical specimens suggest that these gene alterations are rarely, if ever, detected in the same glioblastoma (von Deimling et al., 1993; Watanabe et al., 1996). In a more recent study, where patient tumors were examined for these gene alterations at a cellular level, it was concluded that glioblastomas with *TP53* mutations frequently contain cells with amplified *EGFR*. However, the tendency of the *EGFR*-amplified cells to exist in isolated clusters at the periphery of p53 mutant tumors was interpreted as indicating that impaired p53 cellular function is not conducive to the development of widespread *EGFR* amplification in GBM (Okada et al., 2003). In the examples shown in the present study, high-level and widespread *EGFR* amplification is seen as being compatible with two distinct *TP53* mutant backgrounds.

The genetic characterization of serially propagated flank xenografts is essential for maximizing the research benefit from these GBM resources. This would not be the case for xenograft models involving direct intracranial injection of patient tumor (Shapiro et al., 1979) or the intracranial injection of patient tumor following short-term culture as spheroids (Engebraaten et al., 1999), because these approaches do not involve the propagation of a renewable tissue resource. Immunocompromised rodents used for the heterotopic propagation and serial passaging of GBMs can be considered as reservoirs for providing a continuing supply of the same tumor. We (Pandita et al., 2004) and others (Jeuken et al., 2000; Leuraud et al., 2003) have shown that genetic alterations identified in xenografts are consistent with those determined in corresponding patient tumors and that these alterations are stable in association with serial passaging. Here, we have shown that flank tumor gene alterations are maintained following tumor transfer to the orthotopic setting. By combining flank tumor genetic characterizations with a procedure for initiating orthotopic xenografts having reproducible growth characteristics in series of mice, this model should prove useful to multiple neuro-oncology research interests, including the testing of targeted therapeutics.

One therapeutic target that is currently of keen interest in treating GBM is Egf receptor (Quang and Brady, 2004; Rich et al., 2004; Sampson et al., 2003), and the system we have described here represents the first orthotopic model for studying *EGFR* amplification in GBM. We anticipate that the development of a xenograft test panel with several *EGFR*-amplified GBMs would facilitate the identification of effective Egf receptor–targeted therapies, as well as an assessment of the importance of tumor *EGFR* status to predicting GBM response to Egf receptor–targeted therapeutics.

Acknowledgment

The GBM cell line LN-382 was the generous gift of Erwin Van Meir of Emory University in Atlanta, Georgia.

References

Aldape, K.D., Ballman, K., Furth, A., Buckner, J.C., Giannini, C., Burger, P.C., Scheithauer, B.W., Jenkins, R.B., and James, C.D. (2004) Immunohistochemical detection of EGFRvIII in high malignancy grade astrocytomas and evaluation of prognostic significance. *J. Neuropathol. Exp. Neurol.* **63**, 700–707.

Antunes, L., Angioi-Duprez, K.S., Bracard, S.R., Klein-Monhoven, N.A., Le Faou, A.E., Duprez, A.M., and Plenat, F.M. (2000) Analysis of tissue chimerism in nude mouse brain and abdominal xenograft models of human glioblastoma multiforme: What does it tell us about the models and about glioblastoma biology and therapy? *J. Histochem. Cytochem.* **48**, 847–858.

Bernsen, H.J.J.A., Rijken, P.F.J.W., Hagemeier, N.E.M., and van der Kogel, A.J. (1999) A quantitative analysis of vascularization and perfusion of human glioma xenografts at different implantation sites. *Microvasc. Res.* **57**, 244–257.

Bigner, S.H., Humphrey, P.A., Wong, A.J., Vogelstein, B., Mark, J., Friedman, H.S., and Bigner, D.D. (1990) Characterization of the epidermal growth factor receptor in human glioma cell lines and xenografts. *Cancer Res.* **50**, 8017–8022.

Filmus, J., Pollak, M.N., Cairncross, J.G., and Buick, R.N. (1985) Amplified, overexpressed, and rearranged epidermal growth factor receptor gene in a human astrocytoma cell line. *Biochem. Biophys. Res. Commun.* **131**, 207–215.

Ekstrand, A.J, James, C.D., Cavenee, W.K., Seliger, B., Pettersson, R.F., and Collins, V.P. (1991) Genes for epidermal growth factor receptor, transforming growth factor alpha, and epidermal growth factor and their expression in human gliomas in vivo. *Cancer Res.* **51**, 2164–2172.

Engebraaten, O., Hjortland, G.O., Hirschberg, H., and Fodstad, O. (1999) Growth of precultured human glioma specimens in nude rat brain. *J. Neurosurg.* **90**, 125–132.

Finkelstein, S.D., Black, P., Nowak, T.P., Hand, C.M., Christensen, S., and Finch, P.W. (1994) Histological characteristics and expression of acidic and basic fibroblast growth factor genes in intracerebral xenogeneic transplants of human glioma cells. *Neurosurgery* **34**, 136–143.

Galanis, E., Buckner, J., Kimmel, D., Jenkins, R., Alderete, B., O'Fallon, J., Wang, C.H., Scheithauer, B.W., and James, C.D. (1998) Gene amplification as a prognostic factor in primary and secondary high-grade malignant gliomas. *Int. J. Oncol.* **13**, 717–724.

Groves, M.D., Puduvalli, V.K., Hess, K.R., Jaeckle, K.A., Peterson, P., Yung, W.K., and Levin, V.A. (2002) Phase II trial of temozolomide plus the matrix metalloproteinase inhibitor, marimastat, in recurrent and progressive glioblastoma multiforme. *J. Clin. Oncol.* **20**, 1383–1388.

Horten, B.C., Basler, G.A., and Shapiro, W.R. (1981) Xenograft of human malignant glial tumors into brains of nude mice. A histopathological study. *J. Neuropathol. Exp. Neurol.* **40**, 493–511.

James, C.D., Carlbom, E., Dumanski, J., Hansen, M., Nordenskjold, M., Collins, V.P., and Cavenee, W.K. (1988) Clonal genomic alterations in glioma malignancy stages. *Cancer Res.* **48**, 5546–5551.

James, C.D., Galanis, E., Frederick, L., Kimmel, D.W., Cunningham, J.M., Atherton-Skaff, P.J., O'Fallon, J.R., Jenkins, R.B., Buckner, J.C., Hunter, S.B., Olson, J.J., and Scheithauer, B.W. (1999) Tumor suppressor gene alterations in malignant gliomas: Histopathological associations and prognostic evaluation. *Int. J. Oncol.* **15**, 547–553.

Jeuken, J.W.M., Sprenger, S.H.E., Wesseling, P., Bernsen, H.J.J.A., Suijkerbuijk, R.F., Roelofs, F., Macville, M.V.E., Gilhuis, H.J., van Overbeeke, J.J., and Boerman, R.H. (2000) Genetic reflection of glioblastoma biopsy material in xenografts: Characterization of 11 glioblastoma xenograft lines by comparative genomic hybridization. *J. Neurosurg.* **92**, 652–658.

Kleihues, P., and Cavenee, W.K. (Eds.) (2000) *Pathology and Genetics of Tumours of the Nervous System.* Lyon: International Agency for Research on Cancer.

Leuraud, P., Taillandier, T., Aguirre-Cruz, L., Medioni, J., Crinière, E., Marie, Y., Dutrillaux, A.M., Kujas, M., Duprez, A., Delattre, J.-Y., Poupon, M.-F., and Sanson, M. (2003) Correlation between genetic alterations and growth of human malignant glioma xenografted in nude mice. *Br. J. Cancer* **89**, 2327–2332.

Libermann, T.A., Nusbaum, H.R., Razon, N., Kris, R., Lax, I., Soreq, H., Whittle, N., Waterfield, M.D., Ullrich, A., and Schlessinger, J. (1985) Amplification, enhanced expression and possible rearrangement of EGF receptor gene in primary human brain tumours of glial origin. *Nature* **313**, 144–147.

Mahesparan, R., Read, T.A., Lund-Johansen, M., Skaftnesmo, K.O., Bjerkvig, R., and Engebraaten, O. (2003) Expression of extracellular matrix components in a highly infiltrative in vivo glioma model. *Acta Neuropathol.* **105**, 49–57.

Okada, Y., Hurwitz, E.E., Esposito, J.M., Brower, M.A., Nutt, C.L., and Louis, D.N. (2003) Selection pressures of TP53 mutation and microenvironmental location influence epidermal growth factor receptor gene amplification in human glioblastomas. *Cancer Res.* **63**, 413–416.

Pandita, A., Aldape, K.D., Zadeh, G., Guha, A., and James, C.D. (2004) Contrasting in vivo and in vitro fates of glioblastoma cell subpopulations with amplified *EGFR*. *Genes Chromosomes Cancer* **39**, 29–36.

Pilkington, G.J., Bjerkvig, R., De Ridder, L., and Kaaijk, P. (1997) In vitro and in vivo models for the study of brain tumour invasion. *Anticancer Res.* **17**, 4107–4109.

Quang, T.S., and Brady, L.W. (2004) Radioimmunotherapy as a novel treatment regimen: ^{125}I-labeled monoclonal antibody 425 in the treatment of high-grade brain gliomas. *Int. J. Radiat. Oncol. Biol. Phys.* **58**, 972–975.

Rana, M.W., Pinkerton, H., Thornton, H., and Nagy, D. (1977) Heterotransplantation of human glioblastoma multiforme and meningioma to nude mice. *Proc. Soc. Exp. Biol. Med.* **155**, 85–88.

Rich, J.N., Reardon, D.A., Peery, T., Dowell, J.M., Quinn, J.A., Penne, K.L., Wikstrand, C.J., Van Duyn, L.B., Dancey, J.E., McLendon, R.E., Kao, J.C., Stenzel, T.T., Rasheed, B.K.A., Tourt-Uhlig, S.E., Herndon, J.E., 2nd, Vredenburgh, J.J., Sampson, J.H., Friedman, A.H., Bigner, D.D., and Friedman, H.S. (2004) Phase II trial of gefitinib in recurrent glioblastoma. *J. Clin. Oncol.* **22**, 133–142.

Sampson, J.H., Akabani, G., Archer, G.E., Bigner, D.D., Berger, M.S., Friedman, A.H., Friedman, H.S., Herndon, J.E., 2nd, Kunwar, S., Marcus, S., McLendon, R.E., Paolino, A., Penne, K., Provenzale, J., Quinn, J., Reardon, D.A., Rich, J., Stenzel, T., Tourt-Uhlig, S., Wikstrand, C., Wong, T., Williams, R., Yuan, F., Zalutsky, M.R., and Pastan, I. (2003) Progress report of a phase I study of the intracerebral microinfusion of a recombinant chimeric protein composed of transforming growth factor (TGF)-α and a mutated form of the *Pseudomonas* exotoxin termed PE-38 (TP-38) for the treatment of malignant brain tumors. *J. Neurooncol.* **65**, 27–35.

Saris, S.C., Bigner, S.H., and Bigner, D.D. (1984) Intracerebral transplantation of a human glioma line in immunosuppressed rats. *J. Neurosurg.* **60**, 582–588.

Shapiro, W.R., Basler, G.A., Chernik, N.L., and Posner, J.B. (1979) Human brain tumor transplantation into nude mice. *J. Natl. Cancer Inst.* **62**, 447–453.

Smith, J.S., Wang, X.Y., Qian, J., Hosek, S.M., Scheithauer, B.W., Jenkins, R.B., and James, C.D. (2000) Amplification of the platelet-derived

growth factor receptor-A (PDGFRA) gene occurs in oligodendrogliomas with grade IV anaplastic features. *J. Neuropathol. Exp. Neurol.* **59**, 495–503.

Taillandier, L., Antunes, L., and Angioi-Duprez, K.S. (2003) Models for neuro-oncological preclinical studies: Solid orthotopic and heterotopic grafts of human gliomas into nude mice. *J. Neurosci. Methods* **125**, 147–157.

Thomas, C., Ely G., James, C.D., Jenkins, R., Kastan, M., Jedlicka, A., Burger, P., and Wharen, R. (2001) Glioblastoma-related gene mutations and over-expression of functional epidermal growth factor receptors in SKMG-3 glioma cells. *Acta Neuropathol.* **101**, 605–615.

Tonn, J.C. (2002) Model systems in neurooncology. *Acta Neurochir. Suppl.* **83**, 79–83.

von Deimling, A., von Ammon, K., Schoenfeld, D., Wiestler, O.D., Seizinger, B.R., and Louis, D.N. (1993) Subsets of glioblastoma multiforme defined by molecular genetic analysis. *Brain Pathol.* **3**, 19–26.

Wang, X.-Y., Smith, D.I., Frederick, L., and James, C.D. (1998) Analysis of EGF receptor amplicons reveals amplification of multiple expressed sequences. *Oncogene* **16**, 191–195.

Watanabe, K., Tachibana, O., Sata, K., Yonekawa, Y., Kleihues, P., and Ohgaki, H. (1996) Overexpression of the EGF receptor and p53 mutations are mutually exclusive in the evolution of primary and secondary glioblastomas. *Brain Pathol.* **6**, 217–223.

Wong, A.J., Bigner, S.H., Bigner, D.D., Kinzler, K.W., Hamilton, S.R., and Vogelstein, B. (1987) Increased expression of the epidermal growth factor receptor gene in malignant gliomas is invariably associated with gene amplification. *Proc. Natl. Acad. Sci. USA* **84**, 6899–6903.